Journal of
Nanoscience and Nanotechnology
Vol. 7, 440–446, 2007

Interfacial Construction of Gold Nanoshells on 3-Aminopropyl Triethoxysilane Modified ITO Electrode Surface for Studying Cytochrome b_{562} Electrochemistry

Aihua Jing, Yong Tan, Yi Wang, Shaohua Ding, and Weiping Qian*

State Key Laboratory of Bioelectronics, Department of Biological Science and Medical Engineering, Southeast University, Nanjing 210096, P. R. China

An interface of gold nanoshells (GNSs) was constructed on the surface of the 3-aminopropyl triethoxysilane (APTES) modified ITO glass substrates by a simple self-assemble method to form the GNSs-coated ITO electrode. UV-vis spectroscopy, scanning electron microscopy (SEM), and cyclic voltammetry were used to characterize the GNSs interface architectures. SEM and UV-vis spectroscopy showed that an interconnected and stable GNSs interface was formed on the APTES modified ITO glass substrate. The cytochrome b_{562} (Cyt b_{562}) was selected to observe electron transfer reactions of redox protein at the GNSs-coated ITO electrodes. Quasi-reversible electrochemistry of Cyt b_{562} was obtained and its electrochemical behaviors were discussed.

Keywords: Gold Nanoshells, ITO Electrodes, Self-Assembly, Electrochemistry, Cytochrome b_{562}.

1. INTRODUCTION

Efficient and durable electronic communication between electrode and redox proteins requires a special tunnel for electrons to traverse freely and rapidly, which has a wide range of applications in mediator-free biosensors, bioreactors, and biofuel cell.[1–9] Numerous modified electrodes have been fabricated to construct such tunnels to achieve a sufficiently high rate of electrochemical conversion in studying the dynamic of redox proteins on the conducting solid support. Widely investigated interfacial architectures include titanate nanotube,[10] polymers,[11–12] carbon nanotubes,[13] macroporous metal materials,[14–16] and polyelectrolyte multilayers,[17] which allow immobilization of relatively large quantities of proteins and promote the direct electron communication of the loading redox proteins by shortening the tunneling path of electrons. Redox proteins at these modified electrodes facilitate relatively faster electron transfer and catalytic activity than that at the bare electrodes.[18–31]

Gold nanoshells (GNSs) are composite nanoparticles consisted of a dielectric silica core surrounded by a thin gold shell. With such core–shell structure, the plasma resonant frequencies of GNSs depend on the geometry of the nanoparticles, i.e., on the relative ratio of the core and shell. Adjusting the fabricating condition, the optical resonances of GNSs can be located in the near infrared region of the spectrum. The unique optical feature of GNSs has had a wide variety of applications including modulated drug delivery, blood immunoassay, imaging and therapy of cancer, and biosensing.[32–42] Gold nanoparticles had been self-assembled into 2D and 3D structures through cross-linker[43] or adhere to 3D frame[44] to obtain increased surface area electrodes in detection of direct electron transfer of protein or enzyme in electrochemistry. But the electron transmission in cross-linker was weaker than in gold nanoparticles inevitably resulting in decreasing of detection sensitivities and the frame might hinder the electron shuttling to certain extent. With the development of self-assembly technique, interfacial architectures of GNSs can be created on the surface of 3-Aminopropyl triethoxysilane (APTES) modified ITO electrode via the complexation between GNSs and amine groups. We expect such a GNSs interface may provide a suitable microenvironment for immobilizing biomolecules and keeping their activity to a great extent due to the outstanding electrical conductivity and biocompatibility of GNSs. However, there has no report on the electrochemical properties of the GNSs-coated ITO electrodes, and the electrochemical behaviors of redox protein adsorbed on the GNSs-coated ITO electrodes are not yet understood in detail. The redox protein

*Author to whom correspondence should be addressed.

 1533-4880/2007/7/440/007 doi:10.1166/jnn.2007.141

cytochrome b_{562} (Cyt b_{562}),[45] an 11.8 kDa monomeric protein, is found in Escherichia coli. This small soluble heme protein coordinates to the heme iron through ligands of methionine 7 and histidine 102 and is an ideal candidate to observe electron transfer reactions of redox protein at the GNSs-coated ITO electrodes.

In this paper, we use self-assembly technique to construct an interfacial architecture of GNSs on the surface of APTES-modified ITO glass substrates to form the GNSs-coated ITO electrode. With such a GNSs interfacial architecture, the prepared electrode has the unique advantages: First, the electrode has nanoscale voids, which provide the friendly microenvironment for protein loading and improve the stability of the entrapped protein molecules; Second, the electrode has a larger surface than a planar gold electrode to load functional biomolecules. Furthermore, cytochrome b_{562} (Cyt b_{562}) was observed to show high sensitive electron transfer reactions on the GNSs-coated ITO electrode. Therefore, the GNSs interfacial architecture provides an attractive tunnel to facilitate charge transfer for protein voltammetry studies and biosensors.

2. MATERIALS AND METHODS

2.1. Reagents and Measurement

Silica colloidal particles of ~110 nm in diameter were obtained from Nissan Chemical Corporation (Japan). Cytochrome b_{562} was the gift from Dr. Fang Yu in Max-Plank-Institute for polymer research in Mainz (Germany). 3-Aminopropyltriethoxysilane (APTES) was obtained from Aldrich. All other chemicals, such as chlorauric acid, phosphate, and perchlorate were of analytical grade unless otherwise indicated. B-R buffered solutions with various pH values (pH 4.10 to 6.09) were prepared by changing the ratio of phosphoric acid, ethanoic acid, metaphosphoric acid, and sodium hydrate. All the solutions were prepared with Milli-Q water.

UV-vis spectra were employed to investigate the optical properties and stability of the GNSs-coated ITO electrode and performed with a Shimadzu UV3150 UV-vis spectrophotometer in a transmission mode. Scanning electron microscopy (SEM) characterization was carried out on a SIRION FEI SEM to observe the morphology of the surface of the GNSs-coated ITO electrode. Electrochemical measurements were performed using a CHI650B electrochemistry workstation (ShangHai CH Instruments Co., China). All experiments were carried out using a conventional three-electrode system with a GNSs-coated ITO electrode as working electrode, a platinum wire as counter electrode, and a saturated calomel electrode (SCE) as reference electrode. Solutions were degassed with nitrogen to remove O_2. The electrochemical impedance measurements were carried out in a solution of KCl (0.1 mol L^{-1}) containing 1.0×10^{-2} mol L^{-1} $K_3[Fe(CN)_6]/K_4[Fe(CN)_6]$ (1 : 1 mixture) as a redox probe at a potential of 0.09 V. The alternative current voltage was 5 mV, and the frequency range was 0.01 Hz–100 kHz.

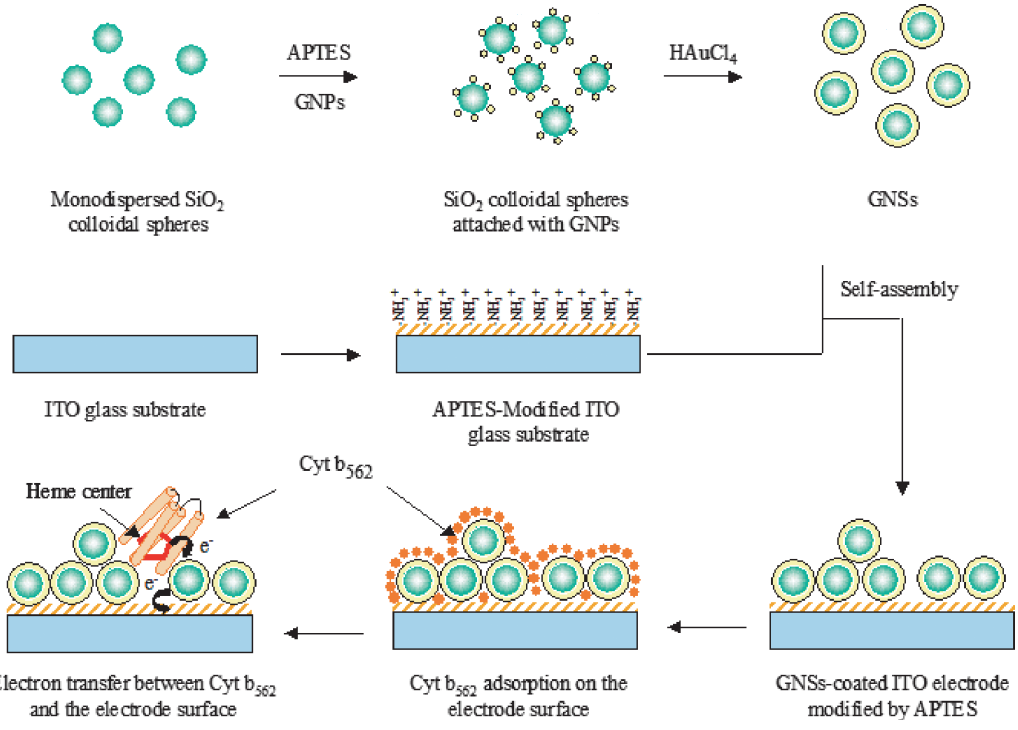

Scheme 1. Fabrication procedure for a GNSs-coated ITO electrode, the process of Cyt b_{562} adsorption on its surface, and the electron transfer between the heme center of Cyt b_{562} and the ITO electrode via GNSs.

2.2. Preparation of GNSs

By reduction of chloroauric acid with sodium borohydride, aqueous suspensions of gold nanoparticles (GNPs) with 2–5 nm in diameter were prepared according to literature procedures with some modifications.[46] Typically, 3 ml of 1% $HAuCl_4$ was mixed with 200 ml of triply distilled water with vigorous stirring, followed by the addition of 1 ml of aqueous solution of K_2CO_3 (0.2 M). Afterwards, 9 ml of $NaBH_4$ (0.5 mg ml^{-1}) was quickly added to the mixture. The wine-red solution was stored at 4 °C until use.[47] GNSs were prepared as described previously.[48–51] APTES was used to functionalize silica colloidal particles.[48] Then, GNPs were attached to APTES-functionalized silica colloidal particles. The attached GNPs served as nucleation sites for the deposition of more gold, resulting in the formation of a complete gold shell on each silica colloidal particle.[50–51]

2.3. Fabrication of GNSs-Coated ITO Electrodes

ITO glass (Xiamen ITO Photoelectricity Industry Co., Ltd., China) was used as a substrate for GNSs-coated ITO electrodes. The ITO glass sheets were sonicated[52] for 30 min in each of the following solvents: soapy water, water and acetone, then were immersed in an ethanol solution of 1% (V/V) APTES for 12 hours. Substrates were rinsed with Milli-Q water and allowed to dry at 120 °C for 3 hours before they were immersed in the solution containing GNSs with a concentration of 1.24×10^{11} particles L^{-1} and form interfacial architectures of GNSs via the complexation between GNSs and amine groups. With this method, GNSs-coated ITO electrode can be fabricated successfully with excellent electrochemical characteristics and stability. The fabrication procedure is shown in Scheme 1.

2.4. Adsorption of Cyt b_{562}

For Cyt b_{562} entrapping, the GNSs-coated ITO electrodes were inserted into the solution containing 1.0×10^{-6} mol L^{-1} Cyt b_{562}. Cyt b_{562} was adsorbed on the gold surfaces of the GNSs-coated ITO electrode via the cysteine or/and NH_3^+-lysine functional groups of the Cyt b_{562}. The process of adsorption of Cyt b_{562} at the GNSs-coated ITO electrode and the electron transfer between them are also shown in Scheme 1.

3. RESULTS AND DISCUSSION

3.1. Spectroscopic and Morphological Characterizations of GNSs-Coated ITO Electrodes

We constructed an interfacial architecture of GNSs on the surface of an APTES-modified ITO glass substrate to form a GNSs-coated ITO electrode. The optical properties and morphology of the electrodes were assessed through UV-vis absorption spectra and SEM. Figure 1 shows the UV-vis spectra of an aqueous solution of GNSs with a concentration of 1.24×10^{11} particles L^{-1} (curve a in Fig. 1) and a GNSs-coated ITO electrode formed in the same solution (curve b in Fig. 1). The characteristic surface plasmon resonance (SPR) peak of the GNSs-coated ITO electrode appeared. The data indicated that the GNSs had been formed on the APTES-modified ITO glass substrate. Figure 2 shows a typical SEM image of the GNSs interfacial architecture on the ITO glass substrate. As can be seen from this SEM image, the GNSs aggregated together to form a cross-linked porous nanoarchitecture.

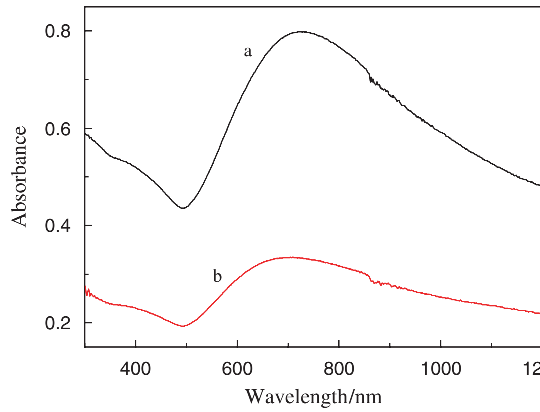

Fig. 1. The UV-vis absorption spectra of GNSs: (a) dispersed in water, and (b) self-assembled on the surface of an APTES-modified ITO glass substrate.

3.2. Electrochemical Behavior of the GNSs-Coated ITO Electrodes

The GNSs-coated ITO electrode was evaluated electrochemically in 1.0 mol L^{-1} H_2SO_4 solution at a scan rate of 0.1 V s^{-1} (Fig. 3). Compared to a bare ITO electrode (Fig. 3, curve 1) with the same geometric surface area, the cyclic voltammograms (CVs) of the GNSs-coated ITO

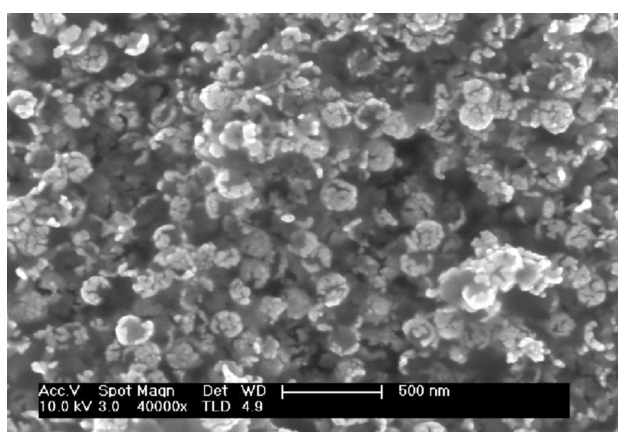

Fig. 2. A typical SEM image of GNSs self-assembled on the surface of an APTES-modified ITO glass substrate.

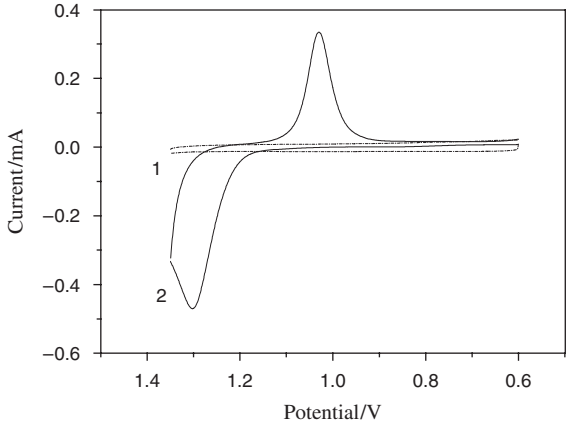

Fig. 3. Cyclic voltammograms of a bare ITO electrode (1) and a GNSs-coated ITO electrode (2) in 1.0 mol L^{-1} H_2SO_4 solution at a scan rate of 0.1 V s^{-1}.

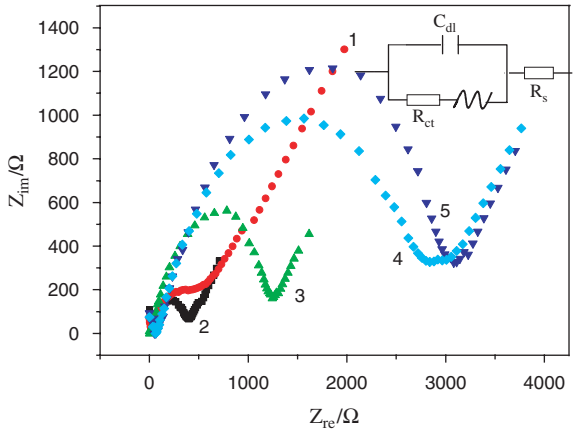

Fig. 4. Nyquist diagrams (imaginary part Z_{re} versus real part Z_{im}) for the electrochemical impedance measurements of electrode in a solution of KCl (0.1 mol L^{-1}) containing $Fe(CN)_6^{3-}$ (1.0×10^{-2} mol L^{-1}), and $Fe(CN)_6^{4-}$(1.0×10^{-2} mol L^{-1}): (1) a bare ITO electrode; (2) a GNSs-coated ITO electrode; (3)–(5) a GNSs-coated ITO electrode with incubating times of 60, 180, and 240 min, respectively, in B-R buffer solution (pH 5.0) containing Cyt b_{562}(1.0×10^{-6} mol L^{-1}). The frequency range: 0.01 ~ 100 KHz, at the formal potential of the $Fe(CN)_6^{3-/4-}$ redox couple and with a perturbation potential of 5 mV. The inset is the Randle's equivalent circuit using a constant phase element instead of capacitance owing to the rough surface.

electrode (Fig. 3, curve 2) showed the oxidation and subsequent reduction waves of the interfacial architecture of GNSs. By integrating the charge required for reducing the gold oxide formed in the positive sweep, the real surface area of the GNSs-coated ITO electrode was determined to be 0.79 cm^2 (assuming that the reduction of a monolayer of gold oxide requires 386 μC cm^{-2}).[53, 54] Compared to the geometrical area of the bare ITO electrode, 0.09 cm^2, the GNSs-coated ITO electrode has a much larger real surface area due to the porous configuration of the interconnected GNSs, which can provide a good microenvironment for the efficient electron shuttle of protein molecules.

3.3. Electrochemical Impedance Spectroscopy

Electrochemical impedance spectroscopy (EIS) was used to obtain the information about the electrical properties of the interface of the GNSs-coated ITO electrode.[55, 56] Figure 4 shows the impedance spectra of the bare ITO electrode (curve 1) and the GNSs-coated ITO electrode (curve 2). The calculated R_{ct} of them were 406 Ω and 385 Ω respectively, indicating the porous structure of the interfacial architecture of GNSs had better effect on the surface electron-transfer reaction than bare ITO electrode. The longer time the GNSs-coated ITO electrode had been immersed in the Britton-Robinson (B-R) buffer solution containing Cyt b_{562}, a higher electron-transfer resistance was obtained, as shown by the enlarged semicircle domains in Figure 4. It illuminated that the Cyt b_{562} molecules had been adsorbed on the surface of the GNSs-coated ITO electrode and the amount of adsorption increased with time. The inset of Figure 4 is the Randles circuit. In the Randles circuit, it was assumed that the resistance to charge transfer (R_{ct}) and the diffusion impedance (W) were both in parallel to the interfacial capacity (C_{dl}). This parallel combination of R_{ct} and C_{dl} gave rise to a semicircle in the complex plane plot of Z_{im} against Z_{re}.

3.4. Electrochemical Behaviors of Cyt b_{562} at the GNSs-Coated ITO Electrode

The electrochemical properties of a GNSs-coated ITO electrode in solution of Cyt b_{562} molecules were examined. Figure 5(A) shows the CVs of a GNSs-coated ITO electrode in a B-R buffer solution (pH 5.0) without (curve 1) and with Cyt b_{562} (curve 2). No redox peaks were observed in the solution absence of Cyt b_{562} while a pair of distinct quasi-reversible redox peaks emerged in the solution containing 1.0×10^{-6} mol L^{-1} Cyt b_{562} due to the direct electron transfer between the adsorbed Cyt b_{562} and the GNSs-coated ITO electrode. A saturated monolayer of Cyt b_{562} on our GNSs-coated ITO electrode was obtained by immersing the electrode in B-R buffer solution of 1.0×10^{-6} mol L^{-1} Cyt b_{562} for 6 hours. Both the anodic and cathodic peak currents of the saturation-adsorbed GNSs-coated ITO electrode increased with the increase of scan rate as shown in Figure 5(B). The inset of Figure 5(B) shows the linear relationship between both the anodic and cathodic peak currents and the square root of scan rate, indicating that the electrode reactions were diffusion-controlled processes.

Figure 6(A) shows the relationship between pH and the peak current of the saturation-adsorbed GNSs-coated ITO electrode. It could see that the peak current increased with pH from 4.0 to 5.0 but decreased with pH from 5.0 to 6.0. The peak current reached a maximum at pH 5.0, just consistent with the isoelectric point (pI) of Cyt b_{562}. The influence of pH on the peak potential of the direct electron transfer of saturation-adsorbed Cyt b_{562} was also observed.

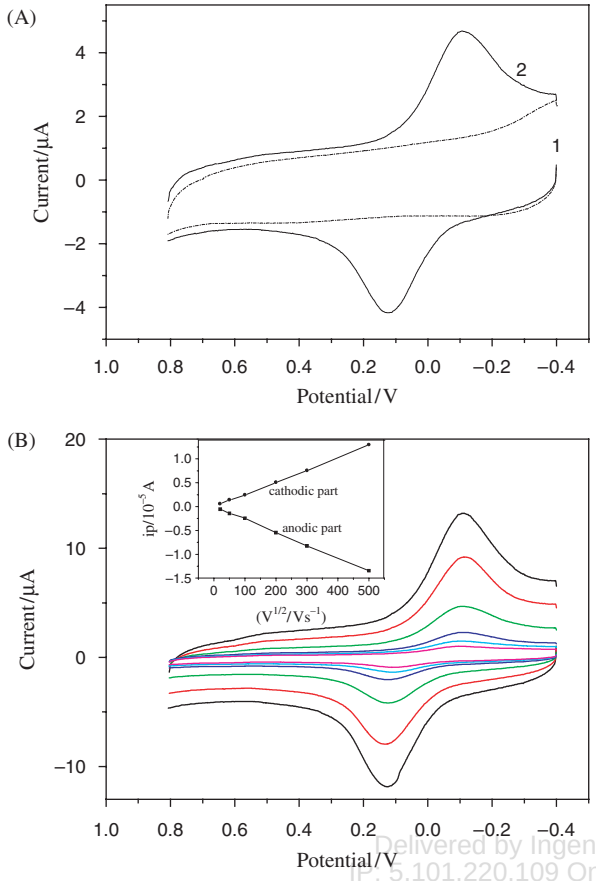

Fig. 5. (A) Cyclic voltammograms of a GNSs-coated ITO electrode in B-R buffer solution (pH 5.0) in (1) the absence and (2) the presence of 1.0×10^{-6} mol L^{-1} Cyt b_{562}, scan rate = 0.05 Vs^{-1} (B) Cyclic voltammograms of a GNSs-coated ITO electrode saturation-adsorbed with Cyt b_{562}(adsorption time: 6 hours) in B-R buffer solution (pH 5.0) containing Cyt b_{562} (1.0×10^{-6} mol L^{-1}) at different scan rates. From inner to outer CVs, the scan rates are 0.02, 0.05, 0.1, 0.2, 0.3, and 0.5 Vs^{-1}. Inset is the plot of the anodic and cathodic peak currents versus (scan rate)$^{1/2}$.

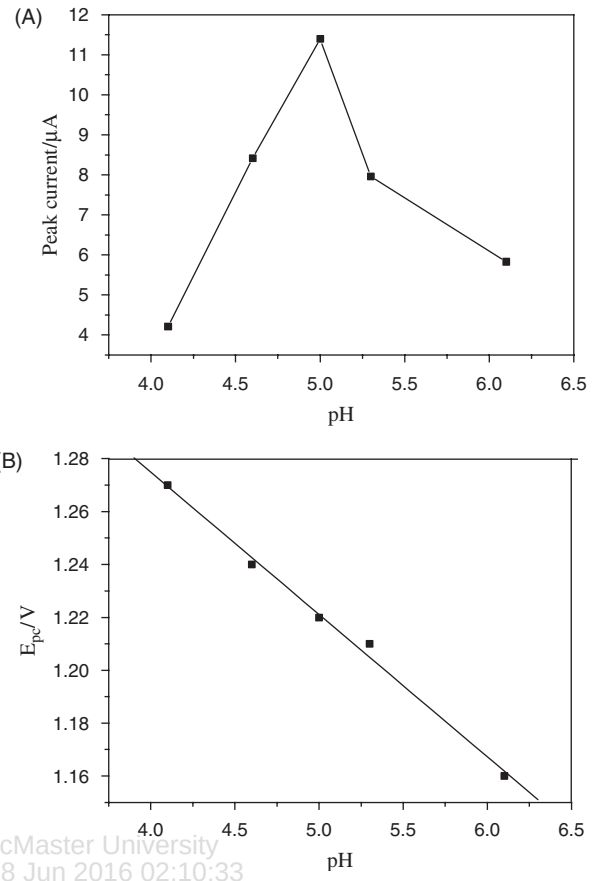

Fig. 6. Influence of solution pH on (A) the cathodic current and (B) the cathodic potential. Dates were obtained from the CVs of a GNSs-coated ITO electrode saturation-absorbed with Cyt b_{562}(adsorption time: 6 hours) in B-R buffer solution containing Cyt b_{562} (1.0×10^{-6} mol L^{-1}). Scan rate = 0.1 V s^{-1}.

Increasing pH caused a negative shift of both the cathodic and the anodic peak potentials. Figure 6(B) shows the relationship between the anodic peak potential and solution pH. A slope of 53 mV pH^{-1} indicated one proton participating in the electron transfer process, which can be represented as Eq. (1):[57]

$$\mathrm{Cyt(Fe^{3+})} + \mathrm{H^+(GNS)} + e^- = \mathrm{Cyt(Fe^{2+})H(GNS)} \quad (1)$$

According to the Laviron equation,[58] the average surface amount (Γ) of Cyt b_{562} can be estimated when a saturation adsorption of Cyt b_{562} on the GNSs-coated ITO electrode at the monolayer level occurred from the slope of the I_p versus ν curve.

$$I_p = \frac{n^2F^2A\Gamma\nu}{4RT} = \frac{nFQ\nu}{4RT} \quad (2)$$

Γ is the surface amount of Cyt b_{562} adsorbed on the GNSs-coated ITO electrode surface (mol cm^{-2}), A is the electrode real area (cm^2), Q is the quantity of charge (C) that calculated from the peak area of the voltammogram, F is Faraday constant, R is thermodynamics constant, T is thermodynamics temperature. The number n of electrons of the direct-electron-transfer reaction of Cyt b_{562} was calculated to be $n = 0.92$, so the redox reaction of the adsorbed Cyt b_{562} on a GNSs-coated ITO electrode was a single-electron-transfer reaction. In addition, the average surface amount of the adsorbed Cyt b_{562} on the three-dimensional GNSs-coated ITO electrode was 5.10×10^{-10} mol cm^{-2}.

When $n\Delta E_p < 200$ mV, the electron-transfer rate constant K_s of Cyt b_{562} on the GNSs-coated ITO electrode can be obtained by Eq. (3).[59]

$$\log K_s = \alpha\log(1-\alpha) + (1-\alpha)\log\alpha - \log\frac{RT}{nF\nu} - \frac{\alpha(1-\alpha)nF\Delta E_p}{2.3RT} \quad (3)$$

Taking the charge-transfer coefficient α of 0.5, the electron-transfer rate constant k_s is 0.62 s^{-1} at a scan rate of 0.1 V s^{-1}.

3.5. Stability of the GNSs-Coated ITO Electrode

To test the stability of the GNSs on ITO glass substrates, we inserted the GNSs-coated ITO electrode into the cuvettes filled with water, ethanol, and benzene in turn prior to performing the spectral measurements. The analysis by the UV-vis spectra (data not shown) shows no discernible difference between pre- and post-immersing, suggesting that the solvents did not cause the GNSs to detach from the ITO glass substrate. The stability of GNSs-coated ITO electrode was also examined by CV experiments. When kept in air for two weeks, the electrochemical signal of the modified electrode decreased by about 5%. After 30 days, the signal decreased by about 10%. This means that the electrode was very stable. Additional, after the Cyt b_{562} saturated GNSs-coated ITO electrode was continuously measured in buffer solution for 3 h, the CV reduction peak current decreased by about 6%. This means that the absorption of Cyt b_{562} on GNSs-coated ITO electrode was stable.

4. CONCLUSIONS

A stable construction of an interface of gold nanoshells (GNSs) on the surface of the APTES modified ITO glass substrates has been prepared by a simple self-assembly method. The characteristics of the GNSs interface were well studied by UV-vis spectroscopy, SEM, and cyclic voltammetry. Effective electron transfer reactions of redox protein were achieved on the interface of gold nanoshells (GNSs) on the APTES modified ITO glass substrates and Cyt b_{562} absorbed on the GNSs-coated ITO electrodes demonstrated direct, quasi-reversible voltammograms. The results indicated that this GNSs-coated ITO electrode displayed good electrochemical characters and showed a much larger adsorption capacity and free orientation possibility of proteins. The favorable electron transfer of a GNSs-coated ITO electrode shows its huge potential use for studying of protein electrochemistry. Work along these lines is now in progress.

Acknowledgments: We thank Dr. Fang Yu (Department of Chemistry, Stanford University, USA) for the Cyt b_{562} sample and many helpful discussions. This research is supported by the National Nature Science Foundation of China (Nos. 20475009, 90406024-4, 60121101), the Nature Science Foundation from Jiangsu province (No. BK2005067), the Foundation from the Ministry of Education, and the Foundation for the Author of National Excellent Doctoral Dissertation of P. R. China (No. 200252).

References and Notes

1. Z. Qiao and S. Dong, *Chinese Univ. Chem.* 14, 1377 **(1993)**.
2. H. Gu, A. Yu, and H. Chen, *J. Electroanal. Chem.* 516, 119 **(2001)**.
3. O. Nadzhafiva, V. Zaitsev, M. Drozdova, A. Vaze, and J. Rusling, *Electrochem. Commun.* 6, 205 **(2004)**.
4. W. Cheng, S. Dong, and E. Wang, *J. Phys. Chem. B* 108, 19146 **(2004)**.
5. G. D. Hale, J. B. Jackson, O. E. Shmakova, T. R. Lee, and N. Halas, *Appl. Phys. Lett.* 78, 1502 **(2001)**.
6. S. Sershen, S. L. Westcott, J. L. West, and N. Halas, *Appl. Phys. B* 73, 379 **(2001)**.
7. S. Mahima, N. K. Chaki, J. Sharma, B. A. Kakade, R. Pasricha, A. M. Rao, and K. Vijayamohanan, *J. Nanosci. Nanotechnol.* 6, 1387 **(2006)**.
8. S. I. Stupp and P. V. Braun, *Science* 277, 1242 **(1997)**.
9. Y. Sun and Y. Xia, *Anal. Chem.* 74, 5297 **(2002)**.
10. M. Wei, I. Honma, and H. Zhou, *Anal. Chem.* 77, 8068 **(2005)**.
11. R. Gabai, N. Sallacan, V. Chegel, T. Bourenko, E. Katz, and I. Willner, *J. Phys. Chem. B* 105, 8196 **(2001)**.
12. Z. Xu, N. Gao, H. Chen, and S. Dong, *Langmuir* 21, 10808 **(2005)**.
13. L. Jiang, C. Liu, H. Li, X. Luo, Y. Wu, and X. Cai, *J. Nanosci. Nanotechnol.* 5, 1301 **(2005)**.
14. C. Wang, C. Yang, Y. Song, W. Gao, and X. Xia, *Adv. Func. Mater.* 15, 1267 **(2005)**.
15. R. Szamocki, S. Reculusa, S. Ravaine, P. N. Bartlett, A. Kuhn, and R. Hempelmann, *Angew. Chem. Int. Ed.* 45, 1317 **(2006)**.
16. E. G. Wijnhoven, S. J. M. Zevenhuisen, M. A. Hendriks, D. Vanmaekelbergh, J. J. Kelly, and W. L. Vos, *Adv. Mater.* 12, 888 **(2000)**.
17. M. K. Beissenhirtz, F. W. Scheller, W. F. M. StÖcklein, D. G. Kurth, H. Möhwald, and F. Lisdat, *Angew. Chem. Int. Ed.* 43, 4357 **(2003)**.
18. J. F. Rusling and A.-E. F. Nassar, *J. Am. Chem. Soc.* 115, 11891 **(1993)**.
19. A. F. Nassar, J. M. Bobbitt, J. D. Struart, and J. F. Rusling, *J. Am. Chem. Soc.* 117, 10986 **(1995)**.
20. R. Lin, M. Bayachou, J. Greaves, and P. J. Farmer, *J. Am. Chem. Soc.* 119, 12689 **(1997)**.
21. N. Hu and J. F. Rusling, *Langmuir* 13, 4119 **(1997)**.
22. M. Bayachou, R. Lin, W. Cho, and P. J. Farmer, *J. Am. Chem. Soc.* 120, 9888 **(1998)**.
23. S. Boussaad and N. J. Tao, *J. Am. Chem. Soc.* 121, 4510 **(1999)**.
24. C. E. Immoos, J. Chou, M. Bayachou, E. Blair, J. Greaves, and P. J. Farmer, *J. Am. Chem. Soc.* 126, 4934 **(2004)**.
25. N. K. Kawahara, W. Ohkubo, and H. Ohno, *Bioconjugate Chem.* 8, 244 **(1997)**.
26. Y. M. Lvov, Z. Lu, J. B. Schenkman, X. Zu, and J. F. Rusling, *J. Am. Chem. Soc.* 120, 4073 **(1998)**.
27. V. Panchagnula, C. V. Kumar, and J. F. Rusling, *J. Am. Chem. Soc.* 124, 12515 **(2002)**.
28. H. Liu and N. Hu, *J. Phys. Chem. B* 109, 10464 **(2005)**.
29. B. R. Van Dyke, P. Saltman, and F. A. Armstrong, *J. Am. Chem. Soc.* 118, 3490 **(1996)**.
30. M. Feng and H. Tachikawa, *J. Am. Chem. Soc.* 123, 3013 **(2001)**.
31. Q. Wang, G. Lu, and B. Yang, *Langmuir* 20, 1342 **(2004)**.
32. L. R. Hirsch, A. M. Gobin, A. R. Lowery, F. Tam, R. A. Drezek, N. J. Halas, and J. L. West, *Annal. Biomed. Engin.* 34, 15 **(2006)**.
33. N. G. Portney and M. Ozkan, *Anal. Bioanal. Chem.* 384, 620 **(2006)**.
34. L. R. Hirsch, J. B. Jackson, A. Lee, N. J. Halas, and J. L. West, *Anal. Chem.* 75, 2377 **(2003)**.
35. P. K. Jain, K. S. Lee, I. H. El-Sayed, and M. A. El-Sayed, *J. Phys. Chem. B* 110, 7238 **(2006)**.
36. C. Wu, X. Liang, and H. Jiang, *Optics Commun.* 253, 214 **(2005)**.
37. C. Loo, A. Lin, L. Hirsch, M. H. Lee, J. Barton, N. Halas, J. West, and R. Drezek, *Tech. Cancer Res.* 3, 33 **(2004)**.
38. J. L. West and N. Halas, *J. Annual Rev. Biomed. Engin.* 5, 285 **(2003)**.
39. J. Jackson, S. Westcott, L. Hirsch, J. West, and N. Halas, *Appl. Phys. Lett.* 82, 257 **(2003)**.
40. C. Radloff, R. A. Vaia, J. Brunton, G. T. Bouwer, and V. K. Ward, *Nano Lett.* 5, 1187 **(2005)**.

41. O. Lioubashevski, V. Chegel, F. Patolsky, E. Katz, and I. Willner, *J. Am. Chem. Soc.* 126, 7133 (**2004**).
42. N. Mano and A. Heller, *Anal. Chem.* 77, 729 (**2005**).
43. M. Lahav, A. N. Shipway, I. Willner, M. B. Nielsen, and J. F. Stoddart, *J. Electroanal. Chem.* 482, 217 (**2000**).
44. L. Wang and E. Wang, *Electrochem. Commun.* 6, 49 (**2004**).
45. J. Okuda, J. Wakai, N. Yuhashi, and K. Sode, *Biosens. Bioelectron.* 18, 699 (**2003**).
46. C. Graf and A. V. Blaaderene, *Langmuir* 18, 524 (**2002**).
47. S. H. Ding, W. P. Qian, Y. Tan, and Y. Wang, *Langmuir* 22, 7105 (**2006**).
48. Y. Tan, S. H. Ding, Y. Wang, A. H. Jing, and W. P. Qian, *J. Nanosci. Nanotechnol.* 6, 262 (**2006**).
49. Y. Tan, S. H. Ding, Y. Wang, and W. P. Qian, *Acta Chim. Sinica.* 63, 929 (**2005**).
50. Y. Lu, Y. Yin, Z. Li, and Y. Xia, *Nano Lett.* 2, 785 (**2002**).
51. G. S. Chai, S. B. Yoon, J. Yu, J. Choi, and Y. Sung, *J. Phys. Chem. B* 108, 7074 (**2004**).
52. W. Cheng, S. Dong, and E. Wang, *J. Phys. Chem. B* 108, 19146 (**2004**).
53. S. Trasatti and O. A. Petrii, *Pure Appl. Chem.* 63, 711 (**1991**).
54. H. Angerstein-Kozlowska, B. E. Conway, A. Hamelin, and L. Stoicoviciu, *Electrochim. Acta.* 31, 1051 (**1986**).
55. E. Sabatani, J. Cohen-Boulakia, M. Bruening, and I. Rubinstein, *Langmuir* 9, 2974 (**1993**).
56. C. Henke, C. Steinem, A. Janshoff, G. Steffan, H. Luftmann, M. Sieber, and H. Galla, *Anal. Chem.* 68, 3158 (**1996**).
57. A. Liu, M. Wei, I. Honma, and H. Zhou, *Anal. Chem.* 77, 8066 (**2005**).
58. E. Laviron, *J. Electroanal. Chem.* 100, 263 (**1979**).
59. E. Laviron, *J. Electroanal. Chem.* 101, 19 (**1979**).

Received: 29 June 2006. Revised/Accepted: 30 August 2006.